IEEE Access
Multidisciplinary | Rapid Review | Open Access Journal

Received May 15, 2020, accepted June 2, 2020, date of publication June 17, 2020, date of current version June 29, 2020.

Digital Object Identifier 10.1109/ACCESS.2020.3002981

Effect of Communication Failures on State Estimation of 5G-Enabled Smart Grid

TESFAYE AMARE ZERIHUN, MICHELE GARAU, AND BJARNE E. HELVIK, (Life Senior, IEEE)
Department of Information Security and Communication Technology, Norwegian University of Science and Technology (NTNU), 7491 Trondheim, Norway

Corresponding author: Tesfaye Amare (tesfayez@ntnu.no)

This work was supported in part by the NTNU Project–Open and Autonomous Digital Ecosystems and CINELDI-Centre for intelligent electricity distribution, an eight year Research Centre under the Research Council of Norway's FME-Scheme (Centre for Environment-Friendly Energy Research under Grant 257626/E20, and in part by the Research Council of Norway and the CINELDI Partners.

ABSTRACT Information and Communication Technologies (ICT), Wide Area Measurement Systems (WAMS) and state estimation represent the key-tools for achieving a reliable and accurate knowledge of the power grid, and represent the foundation of an information-based operation of Smart Grids. Nevertheless, ICT brings new potential vulnerabilities within the power grid operation, that need to be evaluated. The strong interdependence between power system and ICT systems requires new methodologies for modeling the smart grid as a Cyber Physical System (CPS), and finally analyzing the impact of ICT failures on the power grid operation. This paper proposes a novel methodological approach that combines Stochastic Activity Networks (SAN) modeling and numerical computation for dependability analysis of a 5G-based WAMS. Internal influences such as component failures and external influences such as rain effect are considered, and the impact of these failures are assessed over the WAMS capability to provide reliable data for performing an accurate power network state estimation. Different state estimation approaches (traditional SCADA and PMU-based algorithms) and weather conditions are compared in terms of mean states estimation error and safety. The results highlight that 5G based WAMS result in a close-to-ideal behavior which enforces the prospect of a future adoption for smart grid monitoring applications.

INDEX TERMS Smart grid, state estimation, dependability analysis, 5G, wide area measurement system, stochastic activity network.

I. INTRODUCTION

The digitalization wave has invested many areas of industry, utilities and services in the last decades. New markets were opened as a result of the new opportunities brought by the information and communication technologies (ICT), that allow a peer-to-peer exchange of information, goods and services [1].

The power system has also been involved in this transition. A growing request of connection to the distribution grid by small size distributed generation (DG) units has been recorded. This trend is mainly due to the spread of cheap technologies for generation and storage of electrical energy, along with the increased sensibility towards an environment-friendly energy generation, and the political incentives for an increasing contribution of renewable energy into the global energy industry.

The associate editor coordinating the review of this manuscript and approving it for publication was Yue Cao.

With the introduction of distributed generation from Renewable Energy Sources (RES), especially in distribution systems, the complexity of power system operation has increased dramatically. The RES power generation is typically difficult to predict, moreover the bidirectional power flow introduces technical and security issues, therefore efficient monitoring, control and protection of the power system becomes critical. In order to deal with these new challenges, ICTs become a fundamental component of the distribution grid.

The exploitation of ICT in power system operation promises to achieve a significant enhancement in the management of the power network, in terms of better performances, reliability and quality of service [2]. In this context, the concept of Smart Grid (SG) implies the transition of the power grid towards a Cyber Physical System (CPS), where the physical system (the power grid) is merged with a cyber system that provides the physical system with computational and communication capabilities.

Information and communication technologies, along with the above mentioned advantages, introduce new vulnerabilities on power systems that may have a crucial impact on the Smart Grid operation. The data gathered by Wide Area Measurement Systems (WAMS) represent the foundation of the information-based operation of Smart Grids. Wrong state estimation may compromise the integrity of Optimal Power Flow (OPF) and threaten the economic and secure system operation [3]. For this reason a reliable communication technology represents the key enabler for allowing the WAMS to guarantee a correct and timely information exchange for the power system operation. Several factors may influence the capability of correctly processing and delivery of the data within a WAMS. These factors can be classified in two main categories:

- External influences: for example the weather conditions for wireless technologies and the orography of the terrain; cyber-attacks can also dramatically affect the behavior of the ICT system, and consequently of the power grid;
- Internal system reliability: on each Smart Grid component (communication links, servers, measurement devices, actuators, etc.) software and hardware failures may occur.

In this context, 5G technologies represent a promising candidate for implementing the communication infrastructure that allows data traffic to be transmitted from measurement devices to control centers in WAMS. In fact, 5G is expected to meet the requirements for a Smart Grid implementation, with highly reliable communication, low latencies, strong security mechanisms to prevent malicious intrusion and high scalability.

Nevertheless, a comprehensive dependability analysis of WAMS is important in order to:

- quantify the impact of the above mentioned external and internal factors that undermine state estimation applications for power systems;
- support decision-making processes in the Smart Grid infrastructure planning.

A. RELATED WORKS

Several articles have analyzed Wide Area Measurement Systems from a dependability point of view.

In [4] Aminifar *et al.* present a methodology for incorporating WAMS malfunctions in power system reliability assessment based on Monte Carlo simulation. The scenarios analyzed show that WAMS network failures, although unlikely, may bring the system to an unobservable state and cause severe cascading events. A Monte Carlo approach is also used in [5], where a wide area monitoring, protection and control (WAMPAC) system is divided into four subsystems: measurement inputs, communication, actuator and analytic execution, and the influence of different components on the overall system reliability is assessed through sensitivity analysis. Zhu *et al.* in [6] address the dependency of Wide Area Monitoring and Control (WAMC) systems on their supporting ICT architecture. Different architectures are compared in a scenario with a PMU based monitoring system, and the reliability of the whole WAMC system is assessed with relation to data loss probability and delay. Rana *et al.* in [7] propose a reliability evaluation of a power system WAMS with a Markov graph theoretic approach. The analysis considers both single component failures and common cause outages and their impact on the overall reliability of the grid. The model proposed takes also into account the variation of the failure rate of different components in WAMS due to aging.

Several works focus on analyzing the impact on power system state estimation in relationship with a specific cause of data loss and corruption, namely cyberattacks. Liu *et al.* in [8] presents how false data injection attacks can be exploited to bypass the existing techniques for bad measurement detection. Cyberattacks can also be used to create topology errors. Ashok and Govindarasu in [9] show how by exploiting the field devices vulnerabilities, corresponding to the critical measurements, it is possible to manipulate the network topology data. These topology errors are also unobservable to bad data detection techniques. The traditional approaches to detect bad data are based on exploiting a high redundancy of measurement data sources, which allow the identification of outliers, and the application of filtering techniques [10]. Nevertheless, these methods hardly apply on distribution level Smart Grids, which typically rely on a relatively low number of measurement points. Weather conditions impact on a WAMC systems, supported by wireless communication technologies, are analyzed in [11]. The analysis is conducted with a co-simulation approach on a rural distribution network served with WiMAX communication, and it shows the high sensitivity of the wireless channel on the distance between antennas and the level of rainfall. Tsitsimelis et el. in [12] investigate the impact of the LTE random access channel reliability on WAMS and, consequently, on the SE accuracy. The study showed state estimation accuracy can be significantly affected by a varying cell coverage range and number of contending devices in the system. Cosovic *et al.* in [13], [14] propose to leverage 5G cellular technologies to enable a distributed state estimation for smart grid. Latency and reliability of distributed state estimation on 5G communication networks are analyzed. The effect of noise on measurement process and communication process that corrupt the measurement vector is also considered.

B. AIM AND CONTRIBUTION

All the articles mentioned in subsection I-A focus on specific issues on the interdependence between communication system and the power grid monitoring. To the knowledge of the authors, this is the first paper that investigates the overall dependability of 5G based wide area monitoring system (WAMS) comprehensively. Both internal influences such as component failures and external influences such

as fading and rain effects are taken into account, in order to analyze what is the impact of communication failures in the accuracy of distribution network state estimation. The main contributions in this paper are summarized as follows:

- A novel methodological approach is proposed, that combines Stochastic Activity Networks (SAN) modeling and numerical analysis, to take into account the continuous and discrete event activities of power system and ICT system, respectively. Based on this method, a simulation tool is developed with the Möbius platform, extended with external C++ libraries developed by the authors.
- The dependability of WAMS for state estimation in an IEEE standard distribution network is investigated. Different state estimation approaches are analyzed and compared by taking into account internal and external sources of failures, such as component faults and environmental conditions. This analysis is performed over a novel 5G communication infrastructure proposed by the authors, and the suitability of this communication technology is analyzed in relation with the wide area measurement system requirements.

C. ORGANIZATION OF THE PAPER

The paper is organized as follows. Section II gives a brief introductory background to monitoring system architectures and state estimation. In Section III, a 5G-based WAMS architecture is proposed, and the modeling assumptions and implementations are explained. Section IV illustrates the study cases, where the 5G architecture provides a communication service for monitoring the state of an IEEE standard distribution network. The performances of the state estimation are examined in relation with different sources of failures. Conclusive remarks and future works are summarized in Section V.

II. MONITORING SYSTEM FOR SMART GRIDS

This section presents some background on WAMS, 5G and state estimation. Readers with relevant knowledge on these areas may consider skipping this section. The review starts with WAMS architecture in subsection II-A followed by a discussion on the communication architectures on power grid monitoring in subsection II-B. A brief introduction on the use of 5G for WAMS is presented in subsection II-C. Finally, Subsection II-D gives a short background on state estimation algorithms used in WAMS.

A. WAMS ARCHITECTURE

Wide Area Measurement System (WAMS) is a system that combines the functions of metering devices with the abilities of communication systems to monitor, operate and control power systems in wide geographical areas [15]. In general, a WAMS system collects data from measurement devices and transmits them through the communication system to the control center, where the data is processed and decisions on the operation of the power systems are made [16].

Utilities have been using Supervisory Control And Data Acquisition (SCADA) systems for many years for monitoring and controlling the power grids. SCADA is a generic name given for a computerized system capable of collecting and processing data of a complex industrial process through long distances, and applying operational controls over it [17]. Typically, SCADA systems gather data from Remote Terminal Units (RTUs) associated with Measurement Devices (MDs) and convey control signals to Programmable Logic Controllers (PLC) and Intelligent Electronic Devices (IEDs) for operating the system. Nevertheless, traditional SCADA systems are not sufficient for a proper monitoring of modern power systems for various reasons. Among these: the collection of measurement values is every 2 to 5 s; only the RMS values are collected; the measurements are not synchronized in time [18].

Phasor Measurement Units (PMUs) allow providing the WAMS with new capabilities in terms of power grid monitoring. PMUs are measurement devices designed to measure positive, negative and zero sequence phasors of voltages and currents. These signals are sampled at a rate of 50 to 60 times per second, and all the measurements are time-stamped using a clock synchronized to the Global Positioning System (GPS) [18]. Compared with traditional SCADA systems based on conventional RTUs, the integration of a large number of PMUs throughout the grid will result in some benefits. First, it will result in better monitoring due to the higher accuracy of PMU measurement; second, there will be faster control actions due to the higher sampling rate of voltage and current waveforms. Furthermore, due to availability of time-stamped data, there will be better handling with disturbances, potential cascade effects and postmortem analysis [19], [20]. Conventional PMUs are used in transmission systems, and are characterized by an accuracy of $\pm 1^\circ$. However, a higher accuracy is needed for distribution systems as they are characterized by smaller angle difference between buses due to smaller X/R ratios. To meet this requirement, μPMUs have recently been developed. They are able to discern angle differences with an accuracy of $\pm 0.01^\circ$ [21], [22].

In Fig. 1 a typical representation of a modern Wide Area Monitoring Control and Protection system is shown. Substation 1 represents a traditional substation, where measurements from traditional metering devices are merged in a RTU and sent to the Distribution System Operator (DSO) control center, where the information is elaborated by the SCADA system. A modern configuration of substation is represented by Substation 2. Metering devices are substituted by IEDs, that individually communicate with the DSO control center. These substations are also provided with PMUs/μPMUs, whose signals may be aggregated by local or remote Phasor Data Concentrators (PDC) and sent to the DSO control center, where this information is stored in databases and/or processed for real time monitoring by Distribution Management System (DMS) algorithms.

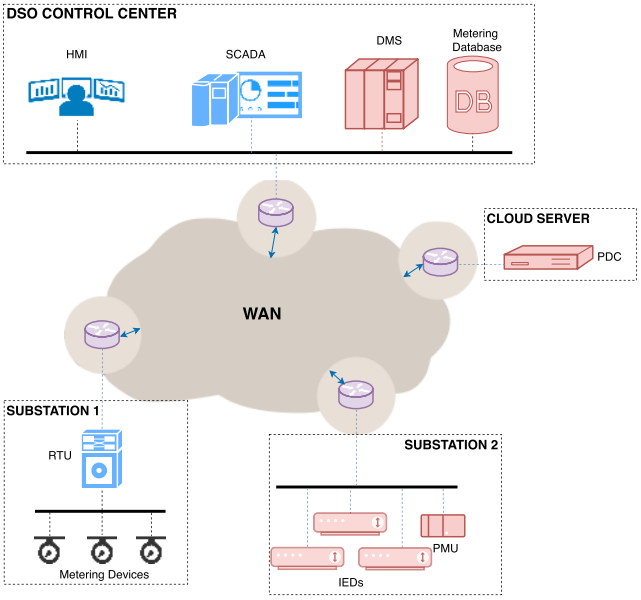

FIGURE 1. Schematic representation of a WAMS: blue blocks represent components of traditional SCADA-based monitoring system; red blocks represent components of modern DMS-based monitoring system.

B. COMMUNICATION ARCHITECTURE

In general, two main levels in the power grid monitoring communication infrastructure can be identified [23]:

- Field Area Network (FAN), that includes the communication of measurement data that is transmitted within the substation, typically between the measurement devices and the RTU.
- Wide Area Network (WAN), that includes the communication of measurement data aggregated at substation level to the central controller, SCADA Master or DMS.

The internal substation communication infrastructure facilitates the communication between the measurement devices and the RTU for substation automation within the same FAN. The RTU collects measurements, alarms, and other information and forwards it to the SCADA system. The most common networking technology within substations FANs is serial communication based on Fieldbus RS-485, that communicate through Modbus, DNP3 or IEC 60870-5-103 communication protocols [24]. The modernization process of substations goes towards replacing these traditional protocols with the newer standard IEC 61850 and introducing a set of abstract models that allow mapping the data objects and services to any other protocol that can meet the data and service requirements. Moreover, conventional RTUs and measurement devices are being replaced with microprocessor-based Intelligent Electronic Devices (IEDs), that support functions formerly supported by multiple conventional devices in the substations. This reduces the cost associated with substation automation and SCADA operation [25]. Compared with previous protocols, IEC 61850 switches from the traditional master-slave communication to a peer-to-peer communication, where all substation devices are IED based and internally communicate through Ethernet LAN. This enables distributed functions as well as data rates up to 100 Mb/s.

The external substation communication infrastructure enables the communication between RTU/IEDs and the SCADA master through the WAN. The state-of-the-art in external substation communication is deployed through Ethernet or Fieldbus RS232, using IEC 60870-5-101, IEC 60870-5-104 and DNP3 protocols. In 2010 the Technical committee TC57 of the International Electromechanical Commission has further extended the standard IEC 61850 to support communication between substations and to support communication between substations and generation sources (IEC 61850-90). With IEC 61850, all substation devices are IED based. Each IED supports one or more functions including switchgears, measurement devices, bay controller and relay. In this stage of modernization of substation automation, each IED will communicate directly with IEC 61850 with the SCADA master over protocols like DNP3, allowing RTUs to be removed. With the advent of IP for SCADA communication, DNP3 has added a Data Connection Management layer, that allows running DNP3 over a TCP/IP or UDP/IP connection. For consistency with IEC 61850 standards, DNP3 will need to support the object models defined in the IEC 61850 standards [18].

Requirements for wide area monitoring communication vary according to the specific application. For example, local voltage stability monitoring, based on conventional metering devices or IEDs, require a typical data sampling with a period of 0.5 to 5 seconds; on the other hand, applications such as real time state estimation or monitoring for supporting power system protection requires data sampling with a period of few milliseconds [26]. IP enabled DNP protocol allow exploiting internet based communication technologies, such as Fiber Optic and broadband wireless technologies (4G and 5G), which are able to meet the low latencies and high reliability required for these monitoring applications [23].

C. 5G COMMUNICATION FOR WAMS

Wireless technologies have already been integrated to SCADA systems for monitoring and remotely accessing the parameters of controlling the substations [27]. Compared with fiber optics, wireless data communication offer significant benefits, such as low cost installations, rapid deployment, easy user access and mobility [28].

Since the 2nd Generation of mobile communication technologies (2G), wireless communication has been successfully tested for monitoring and accessing the performance of remotely situated devices [28], [29]. Nowadays, vendors develop and implement 4G-LTE SCADA connectivity devices, designed to provide several security features like uniquely addressed devices, cryptographic capability, in addition to communication speed [30].

The 5th Generation (5G) of mobile communication technologies represents not only an enhancement of 4G-LTE, but entails a complete redesign of the architecture that supports wireless cellular communication. The 5G, whose first release

has been made available since 2020, is designed to meet the growing demand to the mobile communication infrastructure in terms of number of connected devices, mobile data volumes, latency, reliability and security. Moreover, a wide scope of different use cases will rely on the 5G infrastructure, like enhanced Mobile Broadband (eMBB), Massive Machine Type Communication (mMTC), and Ultra Reliable and Low Latency Communication (URLLC) for Mission Critical Services (MCS), each of which with different and specific requirements [31]. Being able to provide a wide range of use cases and services cost-efficiently requires a high flexibility and a high scalability of the network, that in the 5G vision is obtained through the softwarization of the network, and the concept of network slicing. A network slice consists of a set of virtual network functions that run on the same physical infrastructure, that can be orchestrated and configured according to the specific requirements requested by the network tenant [32]. The key technologies that allow implementing the concept of network slicing are [33], [34]:

- Software Defined Networking (SDN): it separates the control plane and data plane of the current network, promoting flexibility and customization of the network.
- Network Function Virtualization (NFV): it replaces the conventional device bound network functions, such as firewalls, load balancers, etc., with conventional off the shelf servers, enhancing flexibility, convergence of heterogeneous appliances, and allowing reduction of operating and capital expenditures.
- Mobile Edge Computing (MEC): it locates cloud-based architectures at the edge of the mobile network, within the Radio Access Network (RAN) and in proximity of the mobile subscribers, allowing low latency, location awareness, more efficient network and service operations, reduced network congestion and minimized data transmission costs.

In the 21st meeting of Working Party 5A of ITU a preliminary draft of document on utility communication system requirements was reported [35]. Different power network applications are classified in terms of coverage, reliability, latency time, bandwidth, security, priority and backup power. A synthesis of the Working Party results related to the WAMS communication are reported on Table 1.

TABLE 1. Network requirements for monitoring communication.

Application	Coverage	Bandwidth	Reliability	Latency
SCADA WAN	Medium	10 - 100 kbps/node	99 - 99.99 %	2-15 sec
SCADA FAN	High	9.6 - 100 kbps/device	99 - 99.99 %	20 ms - several minutes
PMU for situation awareness	High	600 - 1500 kbps/node	99.999 - 99.9999 %	20 ms - 200 ms

5G technologies promise to meet these requirements. Network Function Virtualization and Mobile Edge Computing allow moving virtual machines with Smart Grid applications and computation capabilities into the edge cloud, reducing the computation delays and enhancing the flexibility and scalability of the system. Ultra Reliable and Low Latency Communication (URLLC) allow meeting requirements, bandwidth and reliability requested for real time state estimation and situational awareness supported by the expected massive deployment of PMUs in distribution grids. Finally, network slicing promises to meet the requirements in terms of security through slice isolation and data encryption.

D. WAMS STATE ESTIMATION

In the Smart Grid (SG) paradigm, measurement systems play an important role. The unpredictability of the power flow, mainly due to the high number of distributed generation units from renewable energy sources (RES) that will be connected to the grid, implies an increasing difficulty in monitoring the state of the network and, based on that, optimally dispatching the resources.

Nevertheless, measurements are prone to errors, due to the precision and accuracy of the measurement devices. State estimation consists in a statistical approach for the calculation of the state variables of the system, given a limited number of measured values characterized by a given uncertainty. Typical measured quantities are the active and reactive power flows on network branches, active and reactive power injections on the buses and voltages on the buses. Recently, the spreading of PMUs and μPMUs enhances the potential of state estimation algorithms with new capabilities, such as prediction of disturbances and potential cascading events, through the measurement of voltage and current phasors and global time stamps [20].

Distribution systems are traditionally a power grid level that is scarcely monitored. A relatively small number of measurement devices is currently deployed along the network compared with the high number of buses. For this reason, pseudo-measurements, i.e. non-real-time measurements obtained from historical data, play an important role for reaching the observability of the system.

The first studies on state estimation algorithms applied to power grids date back to early 70s [36]. In the following years state estimation, due to the evolution of the algorithms, has become a fundamental tool for Transmission System Operators (TSO), and in recent years even for Distribution System Operators (DSO), allowing a continuous monitoring of the power grid and supporting network management interventions.

Several algorithms have been elaborated that allow obtaining an estimation of the state of electrical power systems. The Weighted Least Squares (WLS) is the most commonly used algorithm for obtaining an accurate estimation of the network starting from a set of measures and pseudo-measures [37].

Given a measurement model of a system described by (1):

$$z = h(x) + e \tag{1}$$

where z is a vector containing measurements (and pseudo-measurements) on the electrical system, $h(x)$ is the function

that relates the network state variables x to the measurements on the system, and e is the measurement error vector.

The WLS approach consists in minimizing the following objective function:

$$J(x) = \sum_{i=1}^{M} w_i \left(z - h(x)\right)^2 \tag{2}$$

where w_i is the weight associated to the i_{th} measurement related to the correspondent variance σ_i (if, as commonly assumed, the measurement errors are independent, $w_i = 1/\sigma_i^2$), and M is the total number of measures and pseudo-measures.

Equation (2) can be formulated in matrix form with the following expression (3):

$$\mathbf{J(x)} = [\mathbf{z} - \mathbf{h(x)}]^T \, \mathbf{W} \, [\mathbf{z} - \mathbf{h(x)}] \tag{3}$$

The non-linear problem can be solved thought iterative methods, like Gauss-Newton methods, with the following formulation (4)

$$\mathbf{G(x_k)\Delta x_k} = \mathbf{H_k^T W} \, [\mathbf{z} - \mathbf{h(x_k)}] \tag{4}$$

where

$$\begin{aligned} \mathbf{G(x_k)} &= \mathbf{H_k^T W H_k} && \text{is the Gain Matrix;} \\ \mathbf{H_k} = \mathbf{H(x_k)} &= \frac{\partial h(x_k)}{\partial x} && \text{is the Jacobian matrix of the measurement function } \mathbf{h(x)}; \\ \mathbf{\Delta x_k} & && \text{is the updating state vector from the } k_{th} \text{ to the } (k+1)_{th} \text{ iteration.} \end{aligned}$$

1) PMU-BASED STATE ESTIMATION

In general it is possible to integrate the measurements from PMUs (and/or μPMUs) in the traditional WLS-based state estimation algorithms with two approaches [38]. The first approach consists in appending the voltage and current measurements from PMUs as additional measurements to the conventional measurements vector. Equation (1) is rewritten in the following form (5):

$$\begin{bmatrix} \mathbf{z_1} \\ \mathbf{z_2} \end{bmatrix} = \begin{bmatrix} \mathbf{h_1(x)} \\ \mathbf{h_2(x)} \end{bmatrix} + \begin{bmatrix} \mathbf{e_1} \\ \mathbf{e_2} \end{bmatrix} \tag{5}$$

where $\mathbf{z_1}$ is the vector containing the measurements from traditional measurement devices, $\mathbf{z_2}$ is the vector that contains real and imaginary parts of the voltage and current phasor measurements from PMUs, $\mathbf{h_2(x)}$ is the set of non-linear equations that relate the measurements with the state vector $\mathbf{x}$, and $\mathbf{e_2}$ is the vector of PMU measurement errors. With this approach, both conventional and PMU measurements are processed together, with an iterative approach as in the traditional WLS method.

The second approach is based on a two stages method, which consists in first processing the measurements set from the standard measurement devices with the WLS method, according to (4), and in a second stage post-processing the result of the WLS state estimation with the data based on the measures from PMUs. One example of this approach is proposed in [38], where the PMU measurement vectors is augmented by the estimated state from the WLS:

$$\mathbf{z_2} = \begin{bmatrix} \mathbf{V_{1r}} & \mathbf{V_{1i}} & \mathbf{V_{2r}} & \mathbf{V_{2i}} & \mathbf{I_{2r}} & \mathbf{I_{2i}} \end{bmatrix}^T \tag{6}$$

where $(\mathbf{V_{1r}}, \mathbf{V_{1i}})$ is the solution from the WLS state estimation, and $(\mathbf{V_{2r}}, \mathbf{V_{2i}})$ and $(\mathbf{I_{2r}}, \mathbf{I_{2i}})$ are the voltage and current measurement vectors from PMUs, expressed in rectangular coordinates. Being $\mathbf{x} = [\mathbf{x_r} \ \mathbf{x_i}]^T$ the solution vector that represents the state of the system (real and imaginary part of the vector in the buses), the authors in [38] show that the solution of the state estimation is a linear problem (7):

$$\mathbf{z_2} = \mathbf{H} \cdot \mathbf{x} + \mathbf{e_2} \tag{7}$$

therefore it can be solved in algebraic form. This approach has the main advantage of not requiring the redefinition of already existing state estimation algorithms in SCADA systems. Moreover, being a linear problem, an algebraic solution is obtained without recurring to iterative solvers. For this reason, this approach has also been adopted in the implementation of the state estimation in the dependability platform developed.

III. MODELING

This section presents the 5G based WAMS architecture proposed in Subsection III-A, and the methodological approach adopted for modeling the smart grid monitoring as a Cyber physical system in Subsection III-B. Then, a top level description of the method along with the characteristics of the tool is presented in Subsection III-C. The details on the components model are described in Subsection III-D.

A. PROPOSED 5G BASED WAMS ARCHITECTURE

Based on the technological evolution discussed in Section II-C, a 5G based WAMS architecture is proposed. The monitoring and control logic are virtualized and moved into an edge cloud in a 5G communication infrastructure. IED and PMU functions (such as conversion of analog measurements to digital) are kept near to field devices while PDC data processing functions and Distribution System Operator (DSO) functions are moved into the edge cloud. A completely isolated end to end network slice is considered, which brings multiple benefits such as improved performance due to interference avoidance from the rest of the network.

The 5G based architecture proposed is shown in Fig. 2. IEDs and μPMUs are assumed to communicate with the base station (eNB) through a radio link where ultra reliable and low latency communications (URLLC) service category in 5G is used. The edge computing cloud provides the virtualized application environment, where virtual machines (VM) are used to host monitoring functions of DSO controllers. A Hypervisor is used to manage and orchestrate multiple virtual machines that run concurrently on the host edge cloud server, while a Software Defined Network (SDN) controller is used to manage the front- and back-haul network.

The timing requirement of a real time monitoring applications, as described in Section II-B, is in the range of few

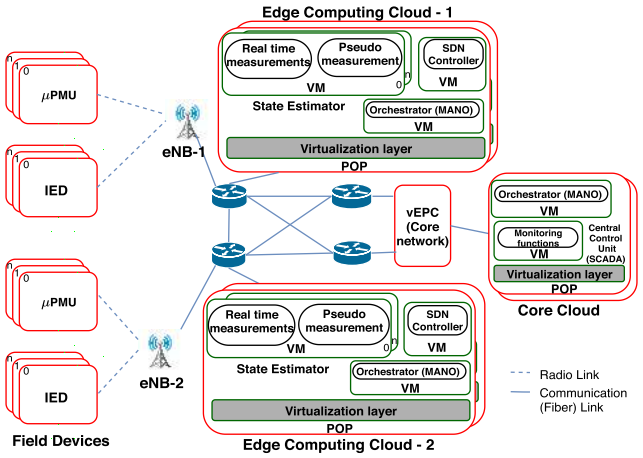

FIGURE 2. 5G based architecture for WAMS.

milliseconds. 5G, by using URLLC radio links and moving the control servers close to the base station (access point), is expected to meet this requirements, with round trip latencies of 1 ms [39].

B. METHODOLOGICAL CHALLENGES IN MODELING SMART GRID

The main issue in studying smart grids as CPS is to allow the two main components of the smart grid, power system and ICT, to be studied comprehensively, despite being two systems with their own peculiar characteristics. More specifically, the power system is traditionally described by mathematical models in the continuous domain. On the other hand, ICT system is typically described with discrete event simulation: the evolution of the ICT system is defined by the sequence of occurring events. In order to properly characterize the smart grid as a CPS, proper attention should be focused on the design of the simulation tool, that must be able to merge these two systems and describe the interdependencies among the elements that compose the complex system (see Fig. 3). This issue brings a methodological

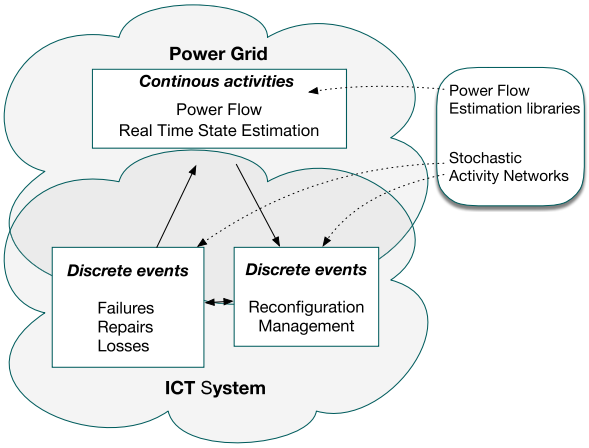

FIGURE 3. Top level methodology description.

challenge, since different exigencies must coexist: on one hand, the necessity of reproducing the operation of the system accurately, on the other hand the need of simplifying the system according to the detail of interest.

C. METHOD AND TOOL

The proposed method follows the principles outlined in Fig. 3. Major events such as failure and repair within power system and ICT systems are modeled along with the ICT infrastructure management (MANO system, VM redundancy, etc.) with the Stochastic Activity Network (SAN) formalism [40]. The power flow and state estimation calculations are performed with numerical solvers.

The SAN models are defined in the Möbius tool [41]. The use of SAN and the tool are extended to allow dealing with continuous phenomena. The main novelty of this extension of Möbius is the inclusion of power system analysis functions by exploiting external C++ libraries purposely developed. In Fig. 4, a schematic representation of the software tool is illustrated.

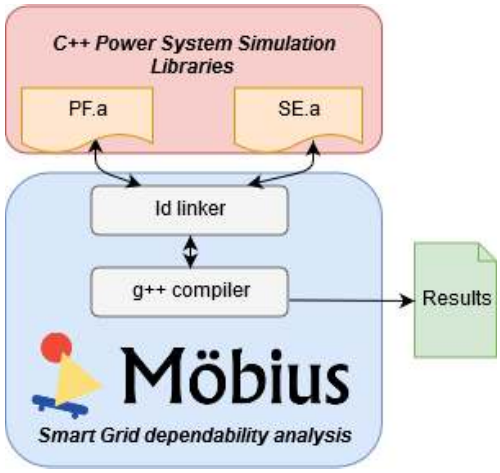

FIGURE 4. Schematic representation of the software architecture of the tool.

The C++ libraries developed for this study are:

- *PF.a*, which provides the tool with the capability of performing power flows;
- *SE.a*, which provides the tool with the capability of performing state estimation calculations.

The simulation is carried out as ordinary discrete event simulation in the Möbius tool, with a modification at the events that may change the power flow. A high level description of the handling procedure of the events is presented in Algorithm 1. Whenever a failure or repair event is generated by the simulation in Möbius, power flow and state estimation calculations are performed. The extensions to Möbius provide the power system analysis functions, defined within the C++ libraries, with the working state of each system component. Based on this information, the power system functions process the data and perform the calculations. Then, the results are collected and recorded as values in the

Algorithm 1 Procedure at Discrete Events in the Simulation

1: Event in the Discrete Event Simulation of the SAN
2: Execute actions in the SAN
3: **if** The event affects the wide area measurements **then**
4: Power flow analysis of new state ▷ PF.a library
5: Store new flow in extended place ▷ Figure 7, ▷ Places: `P_fr`, `VA_fr`, `P_bus`, `VA_bus`
6: Perform State Estimation ▷ SE.a library
7: **if** PMU-based State Estimation **then**
8: Perform PMU-based post processing
9: **end if**
10: Accumulate state estimation statistics
11: **end if**
12: Update the event list
13: Next event in the simulation, i.e. goto line 1

extended places in Möbius, and might be acted upon in further simulations. Extended places are special elements in the SAN formalism of Möbius that allows the model to handle the representation of structures and arrays of primitive data-types (places).

The tool implemented exploits and enhances the inherent advantages of Stochastic Activity Networks formalism:

- *Efficient simulation*: during the simulation, power flow and state estimation calculations carried out only after events change the ICT system topology and/or the power flows. Results for a given configuration are cached to avoid repetitive calculations of normal conditions, shortening the simulation time;
- *Structured modeling*: each type of component of relevance in the power grid and ICT system is modeled with an atomic model. The interconnection between components is embedded in the input/output gates and extended places. This approach simplifies the description of the system and the interdependencies that exist between the system components;
- *Modularity and flexibility*: the model is easily extendable with new features; the introduction of new atomic models and refinement of existing allow upgrading the smart grid definition with an enhanced level of details. Furthermore, the exploitation of external libraries allows modeling the dynamics of the system such as introducing power system analysis capabilities and other active management functionalities (network operation strategies, transient simulation analysis, etc.).

D. MODEL DESCRIPTION

Based on the 5G based architecture proposed in Section III-A. The model is based on the principles of object orientation. First, a Möbius atomic model is developed for all types of components of the architecture describing their generic behavior. Next, these types are instantiated, i.e. given parameters and variables, to represent the specific individual components of that type in the system. The instances and the system topology are represented using an indexed extended place in the atomic models. Then, the overall system is modelled by connecting the atomic sub-models. The reward model functionality in Möbius is used to collect statistics of interest for each state transition of the system (failures and repairs). Below, some important atomic model types for the 5G architecture are presented. For a more detailed description of the atomic models, refer to [42].

1) EDGE INFRASTRUCTURE

Figure 5 shows the atomic model of an edge server. It has four extended places: hardware failure (`Server_Failed`), working state (`Server_Ok`), Operating system/Software failure (`Soft_Failed`) and No Power states (`No_Power`). The states of the servers are modeled by markings of the respective extended places. The atomic model for virtual machine is shown in Fig. 6. A virtual machine may have a software failure (`VM_Sf_Fail`) or a failure in the underneath edge server may change its state into a hardware failure state in `VM_Hr_Fail`. The unconnected extended places at the top are shared places, which are used to share states with other atomic models.

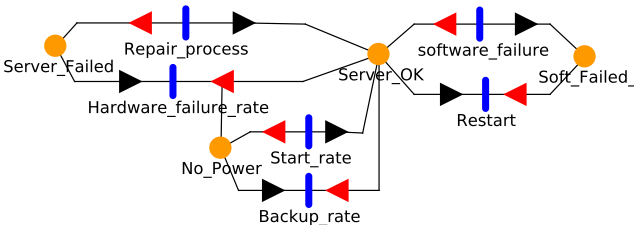

FIGURE 5. Atomic model of the server.

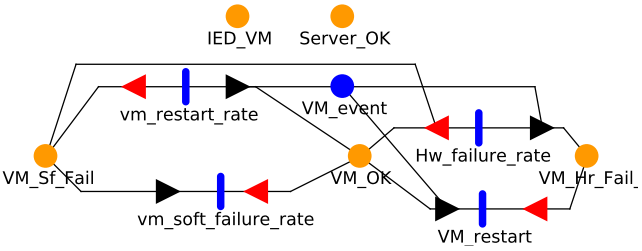

FIGURE 6. Atomic model of virtual machine.

2) ESTIMATOR APPLICATION MODEL

The estimator application atomic model, shown in Fig. 7, contains the core setup for the exchange of information between the ICT system and power system models as discussed in Subsection III-C. It consists of three places: `OK_Initial`, `Estimation` and `Failed`. The global variables, defined as extended places, are exploited for storing the power system variables from both the power flow analysis and state estimation. A power flow analysis is made on the initial state prior to estimation so that the ideal case values are known.

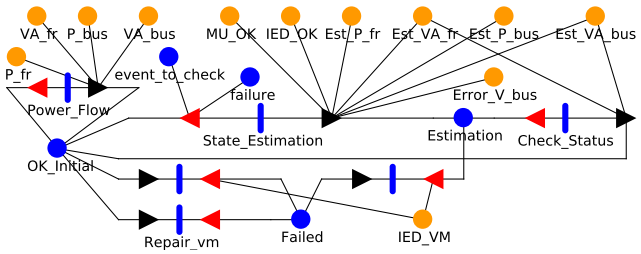

FIGURE 7. Atomic model of estimator application.

The remaining places `failure` and `event_to_check` are shared with other monitoring system components such as the measurement devices. According to discrete event simulation paradigm, these shared states are used to trigger the state estimation calculation. Both the power flow and estimation libraries are called in this atomic model and the results are stored in the respective global power system variables. The estimator application may turn from working states (`OK_Initial` and `Estimation`) to a failure state (`Failed`) if the underlying virtual machine fails to provide service (through `IED_VM`).

3) FIELD MEASUREMENT DEVICES

The atomic model for field measurement devices, such as μPMUs or IEDs, is shown in Fig. 8. It consists three extended places: hardware failure (`Sensor_Failed`), working state (`Sensor_OK`) and loss of communication `Sensor_No_Comm`. A field measurement device will be unavailable if it either has a hardware failure or if the radio communication to the eNB is lost. The state of the radio communication is monitored through the shared extended place `Com_OK`. The state of the field device measurement will finally be communicated to the estimator through the shared place `event_to_check` and `failure`.

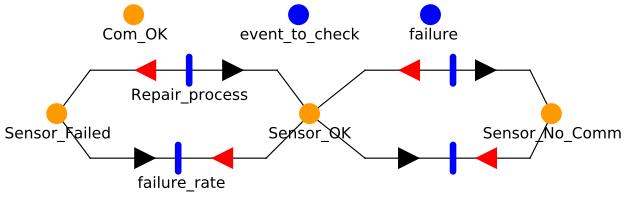

FIGURE 8. Atomic model of field measurement device.

4) RADIO COMMUNICATION

The radio communication represents the most vulnerable part of WAMS. For this reason, a detailed model of the radio communication subsystem is developed. In addition to conventional component failures, a special focus is put on environmental factors such as signal fading and rain effect. The model assumes that each field component (SCADA measurement device or μPMUs) is connected to the eNB through a single homed radio communication channel. It is also assumed that each radio communication channel consists of multiple paths (n radio signals).

The radio subsystem model is structured in three stages, which will be discussed separately. First, an atomic model for reliability of the wireless channel modeling the multi-path fading on the n redundant signals of a single radio communication channel. Next, the atomic model of the radio communication that includes the radio channel together with hardware equipment is introduced. Lastly, the modeling of rain effect on the radio channel reliability is discussed.

a: RADIO CHANNEL MODEL

The radio channel is typically characterized by either a large-scale fading or a small scale fading. The large scale fading is due to the path loss and shadowing while the small scale fading is due to the constructive and destructive interference of the multiple signal paths [43], [44]. Though the model developed is exploitable to analyze both properties, the model proposed ignores path loss and shadowing, assuming a compensation is performed by controlling the transmission power. Considering urban areas where there can be many moving objects that may scatter the n radio signals on their way to the receiver, a Rayleigh model is assumed for capturing the effect of small-scale fading.

For reliability studies, the fading behavior of the radio transmission can be considered as an alternating renewal process with failure (λ) and recovery (μ) rates where the failure of the transmission is attributed to the fading. The average fading and non-fading duration of a Rayleigh-faded signal can be determined by level crossing analysis as discussed in [43], [44]. Their reciprocals characterize the transition rates between a working state and a failure state, which is denoted as failure rate λ and recovery rate μ as shown in (8):

$$\lambda = \sqrt{\frac{2\pi}{F}} f_{\mathrm{D}}, \quad \mu = \frac{\sqrt{\frac{2\pi}{F}} f_{\mathrm{D}}}{\exp \frac{1}{F} - 1} \tag{8}$$

where $F = p_{\mathrm{avg}}/p_{\mathrm{min}}$ represents the fading margin with the average receive power p_{avg}. The maximum Doppler frequency is characterized by $f_D = vf/c$, where f is the carrier frequency of the signal and c is the speed of light. The relative velocity between transmitter, receiver, and scatterers is denoted by v. In smart grid environment, the transmitter and receiver are stationary. Nevertheless, there can be a minor effect from scatters especially in urban areas. Hence, the model assumes a small fraction of the failure due to fading (r) where $f_D = (vf/c) \cdot r$.

The first stage atomic model in Fig. 9 is used to study the wireless channel property (i.e. the short term fading behavior). It consists two extended places; working (`Radio_signal_Ok`) and failure due to fading (`Radio_signal_Failed`). The markings in the two extended places represent how many of the n radio signals are (not-)working. A radio channel is assumed to be viable as long as one out of the n redundant signals is operational. The radio channel is said to be failed if all n tokens are present

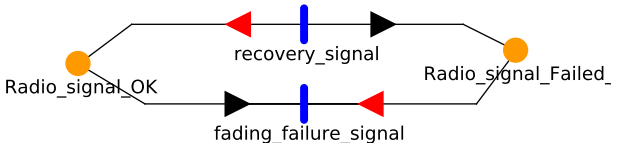

FIGURE 9. Atomic model of a fading radio channel.

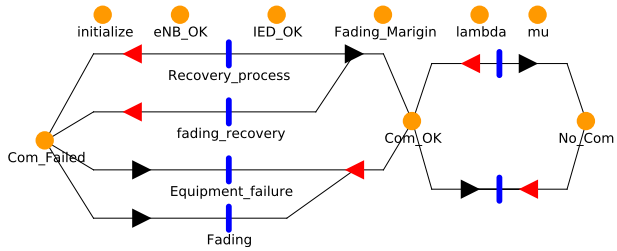

FIGURE 10. Atomic model of the radio communication.

in `Radio_signal_Failed`. The rates of transitions, `fading_failure_signal` and `recovery_signal`, are obtained from the λ and μ of (8). The model measures the rate at which the radio channel fails (all signals are down) due to fading and get recovered by tracking the number of visits to the failure state.

b: RADIO COMMUNICATION

The second stage radio communication model, shown in Fig. 10, is used to model the radio communication as a single entity, including the radio channel together with hardware equipment. This model is suited for studying the availability of communication between sensors and the radio tower. It consists of three extended places: Working (`Com_Ok`), No communication due to failure on ICT components (`No_Com`) and link failure (`Com_Failed`). The failure of a communication link has different states represented by different marking of the extended place. It could be due to hardware failure on the receiver and transmitters which need maintenance by a recovery crew, or due to fading with a failure rate obtained from the first stage model.

c: RAIN EFFECT MODEL

In addition to the small-scale fading, the attenuation due to rain precipitation is considered. In fact, similar to small-scale fading, rain precipitation is an event that rapidly changes the attenuation between base station and user equipment. Therefore, no compensation from the base station can occur and the rain may cause communication failure. The effect may be pronounced in areas where the rainfall intensity reaches high values in large parts of the year.

In this study Norway has been considered. According to ITU recommendations, Norway is described by four rain regions that differ in terms of distribution of rainfall intensity over the year [45], [46]. The four regions considered (C, E, G, J) are reported in Table 2 with the corresponding rainfall distribution.

TABLE 2. ITU-R rain rates for map regions of Norway.

% of year exceeded	Rainfall rate exceeded (mm/h)			
	C	E	G	J
0.001	42	70	65	55
0.003	26	41	45	45
0.01	15	22	30	35
0.03	9	12	20	28
0.1	5	6	12	20
0.3	2.8	2.4	7	13
1	0.7	0.6	3	8

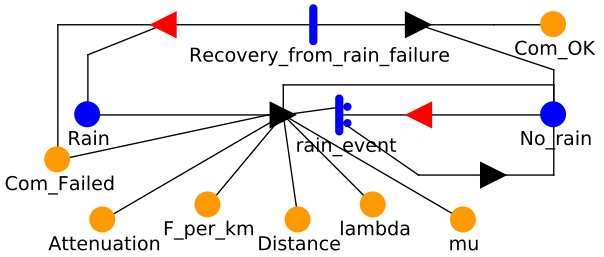

FIGURE 11. Atomic model of rain effect.

The attenuation Γ_R (dB) is obtained from the rain rate R (mm/h) using (9):

$$\Gamma_R = k \cdot R^{\alpha} \cdot d \tag{9}$$

where k and α are two coefficients that depend on polarization and frequency, and d is the distance between the considered node and the nearest base station.

The attenuation Γ_R reduces the fading margin available for the small-term fading F in (8). Given F^* as the maximum fading margin in the radio link, the actual fading margin value will be given by (10):

$$F = F^* - \Gamma_R \tag{10}$$

A Möbius atomic model for modeling the rain effect is presented in Fig. 11. It has two places: Rain (`Rain`) and No rain (`No_rain`). The markings in the two places represent the condition when the rainfall results in a significant attenuation or if it results in a negligible attenuation that does not affect the signal transmission. A rainfall rate of 3 mm/h has been considered as threshold for the transition between these two states. When a rain event exceeding the threshold occurs, the resulting attenuation for each radio channel is calculated according to (9) and stored in `Attenuation`. Then, the remaining fading margin is calculated according to (10), and the failure and recovery rates (`lambda` and `mu`) of the radio channel model (Fig. 10) are updated accordingly. For those radio channels with attenuation exceeding the fading margin, the radio channel is considered failed (through `Com_Failed`). When the rainfall ends, all the radio channel states are restored to their default state.

IV. DEPENDABILITY ANALYSIS

The study investigates the dependability of the proposed 5G communication infrastructure of WAMS in distribution grid.

A comparative analysis, that considers different assumptions and configurations of the 5G infrastructure, is conducted with the simulation tool introduced in Subsection III-C.

A. CASE STUDY

A simulation study of a distribution network is carried out, focusing on measuring the impact of ICT failures on the state estimation of the grid.

1) POWER GRID

The analysis is performed on the IEEE 33-bus standard distribution network (Fig. 12). It is a 12.66 kV radial network that feeds approximately 3.6 MW of peak active power load and 2.2 MVAR of peak reactive power load [47]. The IEEE 33-bus standard network considers normally open emergency ties that allow reconfiguring the network when failures occur. In the future distribution networks, with a high penetration of distributed generation, will increasingly be operated in weakly meshed topology [48]. Therefore, in this study, the disconnectors that maneuver the emergency ties (dotted lines) are considered normally closed, i.e. the distribution network operates in a meshed configuration. The bus 1 is assumed as the slack bus, with reference voltage 1 pu. Power flow calculations return the voltage profile over the 33 buses, which are within the normal operation range for distribution networks of $0.95 \div 1.05\, pu$ [49].

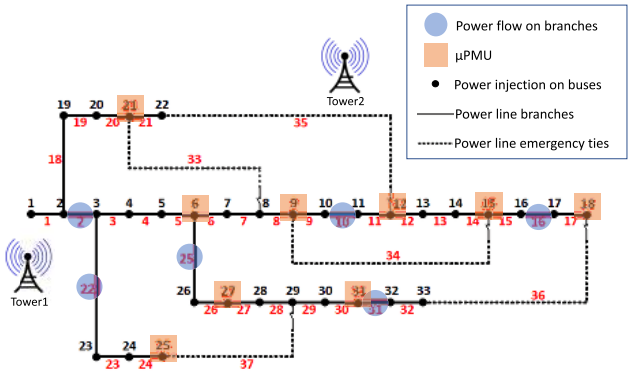

FIGURE 12. IEEE 33-bus standard distribution network.

A mix of bus power injection measurements, branch power flow measurements and μPMU measurements are deployed along the network. The Wide Area Measurement System is implemented with IEDs or μPMUs, that communicate directly to the SCADA master and DMS located at the DSO control center, according to a centralized architecture. The IEDs and μPMUs placement is done ensuring that the power system is fully observable whenever any measurement unit is interested by a failure (N-1 approach).

The IEDs transmit the measurements of bus power injections and branch power flows to the SCADA master every 2 seconds, and then a robust SCADA+PMU state estimation calculation is performed. μPMUs transmit voltage and current phasor measurements every 100 ms to the DMS. The DMS post-processes the previous state estimation with the updated μPMUs measurements, exploiting the two-stages linear state estimation approach explained in subsection II-D1. An example of the approach followed is represented in Fig. 13.

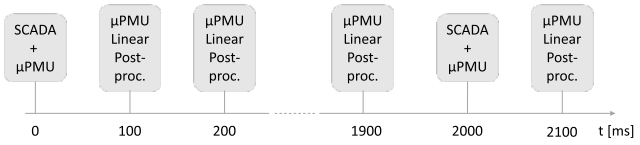

FIGURE 13. State estimation SCADA + PMU processing synchronization.

2) ICT SYSTEM

The 5G architecture proposed in subsection III-A is studied, which assumes that the measurement points are connected to the estimator application on the edge cloud through a radio access network, see Fig. 2. Two radio towers are located in the proximity of the power grid and each sensor is provided with a 5G User Equipment which is connected to the nearest tower. To each of these components (IEDs, μPMUs, UE, Base Station) an instantiation of the correspondent atomic models (ref. III-D) is associated. For a description of the instantiation process, see Subsection III-D. An atomic model is also instantiated for each communication link between UEs and nearest base station. Finally, an atomic model is instantiated for each component of the 5G Edge Computing Cloud and Core Cloud (Fig. 2), namely the server, the virtual machine, the estimator application. For a complete list of 5G architecture model, see Subsection III-D. All these atomic models are merged with the Join feature of the Möbius tool. For the sake of brevity, the authors refer the reader to [50], [51] as example of application of SAN atomic models for ICT system modeling in different distribution systems.

All the transitions (i.e., Failure events, repair events, rain occurrence, etc.) in each atomic model are assumed with a constant failure rate, yielding negative exponentially distributed firing times T_x, i.e. $P(T_x > t) = e^{-\lambda_x t}$, for transition x. The usage of negative exponential distribution for repair and recovery times is due to the lack of empirical information about the distribution of these events, combined with the lack of sensitivity in the results to their distribution. This is considered a fair assumption, as long as the repair and recovery times are short compared to the time between failures. Table 3 presents the failure rates and repair times used in the numerical evaluation. For edge computing server components these are based on [52] and [53], while the parameters used for the field devices are from [54].

3) METRICS

The following metrics are used to quantify the impact of communication failures on the accuracy of the state estimation of the power grid:

- Mean Estimation Error (MER) – $\bar{E}(x)$: measures the difference between the estimated power system state

TABLE 3. Failure rates and recovery times of the system components.

Component type	Failure rate [days^{-1}]	Mean recovery time [hr]
RTU / μPMU	$2.6 \cdot 10^{-3}$	2
Fiber Line	$6 \cdot 10^{-6}$	6
Router/Switches	$5 \cdot 10^{-3}$	3
Host server (permanent failures)	$4.9 \cdot 10^{-3}$	2
Host OS (Software failures)	$1.667 \cdot 10^{-2}$	1 (repair) $1.667 \cdot 10^{-1}$ (reboot)
Virtual Machine Monitor	$8.3 \cdot 10^{-3}$	1 (repair) $1.667 \cdot 10^{-1}$ (reboot)
Virtual machines	$1.1 \cdot 10^{-2}$	1
eNB	$2 \cdot 10^{-4}$	10
Power supply failure	$1.9 \cdot 10^{-3}$	3
Radio Link	$8.64 \cdot (10^{0}$–$10^{1})$	$2.77 \cdot 10^{-4}$ (=100ms)

variable x using WAMS and the ideal/actual values obtained with power flow calculation. In the following study cases, the state variable x considered is the bus voltage magnitude. The mean estimation error is measured for each bus in the power grid network. The mean of the estimator error for all buses is also considered as metric.

- Safety – $\bar{S}(x)$: represents the probability that the estimation error is greater than a certain critical threshold value, TR. It gives information about the probability that the estimation error triggers a decisive and critical action by the control unit.

4) STUDY CASES

The study aims at assessing the dependability of the two different state estimation algorithms introduced in Subsection II-D. The study investigates first the degree of vulnerability of the different subsystems of the WAMS architecture, then the impact of component failures over the state estimation accuracy is analyzed in detail. The study is divided in the following cases:

A: The influence of the different 5G-based WAMS subsystems (Sensors, Radio access, eNBs and Edge cloud) on the reliability of state estimation calculations is analyzed.

B: The 5G configuration with a SCADA based state estimation (SCADA-SE) is studied and compared with a WAMS setup with ideal communication. Two sub-cases are considered:
B.1: The SCADA-SE with a closer look at the radio subsystem (the environmental impact due to rain) is considered. The effect of failure in communication due to rain on the state estimation performances is investigated. Four map regions (C, E, G and J) of the ITU-standard (2) that fall into the area of Norway are considered.
B.2: The SCADA-SE with a focus on the sensor subsystem is considered. The effect of different recovery strategy for sensors is studied. The following three strategies are considered; immediate repair, differing recovery until two sensors are failed, and differing recovery until three sensors are failed.

C: The impact of communication failures on state estimation MER and safety is analyzed in the WAMS setup with PMU-based linear post-processing of SCADA measurements.

In all case studies, the safety metric has been considered associated with a voltage threshold $TR = 0.02\,pu$. Therefore, it has been assumed as critical state the condition when the estimation error exceeds $\pm 2\%$ of the actual voltage value. Moreover, in the case of losing information due to failures, the estimator algorithm uses pseudo-measurements taken from the historical data. Except for the case in which the four rain-regions are specifically compared, we assume region G as default region in all cases, corresponding to the most severe scenario (details are provided in the discussion of case B.2 in subsection IV-B).

All cases are simulated for 1 year of calendar time, each replicated 15 to 20 times to achieve a sufficient statistical confidence level of the simulation results. In the result presented below, the ratio between the 95% confidence interval of the estimates and the estimate are 3% to 8%.

B. EVALUATION AND DISCUSSION

For all cases mentioned in Section IV-A4, a simulation of the operations of the network, including failures, repairs, transmission problems, etc., is run with WLS State Estimation (4) calculated every 2 seconds with SCADA-based WAMS. For the case where μPMUs are considered, every 100 ms the results are refined with the PMU-based linear state estimation algorithm (7).

Case A: The effect of failures on the different subsystems is first analyzed by measuring the unavailability of each subsystem. A subsystem is considered unavailable if one or more component in the subsystem fail, assuming it may affect the estimation process. In this analysis, measurements are taken provided that a failure occurs in the considered subsystem.

Fig. 14a shows the unavailability measure of the four major subsystems of the 5G based WAMS architecture: set of sensors, radio channel, radio towers (eNBs) and edge cloud. It can be observed that the measurement devices (sensors) introduce the highest contribution to the total unavailability, followed by the radio access subsystem. The eNBs and the edge cloud have a very small contribution to the system unavailability, 10^{-4} and 10^{-7} respectively.

Fig. 14b shows the impact of the different subsystems on the WAMS dependability in terms of MER and safety metrics. The radio subsystem, although characterized by a lower unavailability figure compared with the sensor subsystem, results in slightly higher mean estimation error and safety values. Failures in the radio access are frequent and characterized by short duration that results in a higher number of simultaneous failures. They therefore affect the performance of state estimator algorithm that results in higher MER.

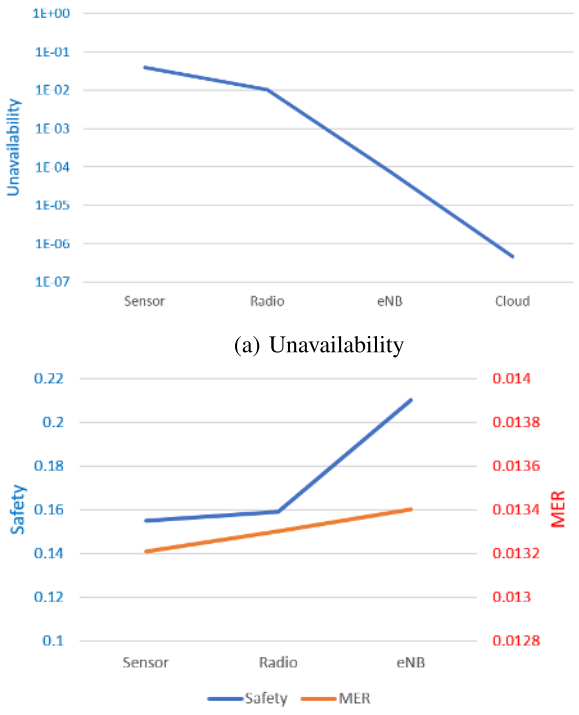

(a) Unavailability

(b) Safety and mean estimation error

FIGURE 14. Comparison of different subsystems in 5G architecture.

Failures in eNBs result in the highest MER. The main reason is the wide impact of failures in eNBs, which result in loss of coverage for a high number of sensors, and therefore a higher uncertainty in the state estimation calculation. Nevertheless, the exploitation of pseudo-measurements mitigate this effect allowing to produce a reasonable estimation. For the same reason, even the safety does not increase consistently compared with the other cases. In Fig. 14b the metrics related to failure on the edge cloud are not reported since failure of the edge cloud would leave the system unobservable.

The following polar diagrams report the analysis of the state estimation accuracy at a bus level. The results of the state estimation are compared with the actual value calculated with the power flow library, and the metrics MER and Safety are calculated for each bus.

In Fig. 15 the impact of failures on the different WAMS subsystems in terms of MER (Fig. 15a) and safety (Fig. 15b) is evaluated on each bus.

Figure 15a shows that the radio channel is the most critical source of mean estimation error compared to sensors and eNBs. Although each failure in the eNBs results in a high MER, the effect seen over a ten-year simulation is small. On the other hand, failures on the radio channel, although singularly characterized by a lower MER impact than the eNBs, result in a higher MER on a longer time scale, due mainly to the higher failure rate. A similar behavior is observed for the safety metrics, but with failures in radio access subsystem resulting in slightly higher safety values only on some buses, such as from bus 9 to bus 16.

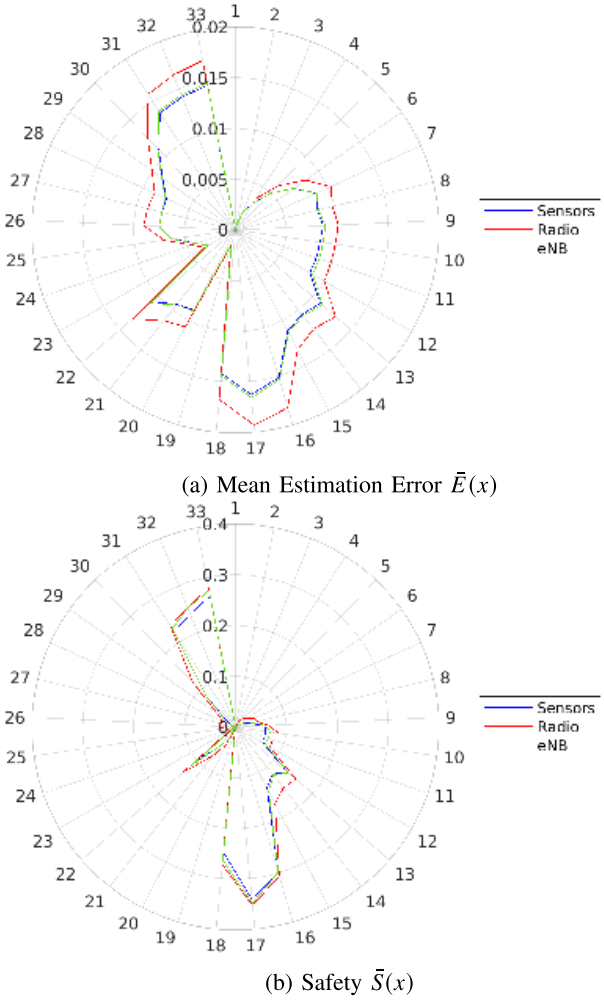

(a) Mean Estimation Error $\bar{E}(x)$

(b) Safety $\bar{S}(x)$

FIGURE 15. Effect of failure in the different subsystems in 5G architecture.

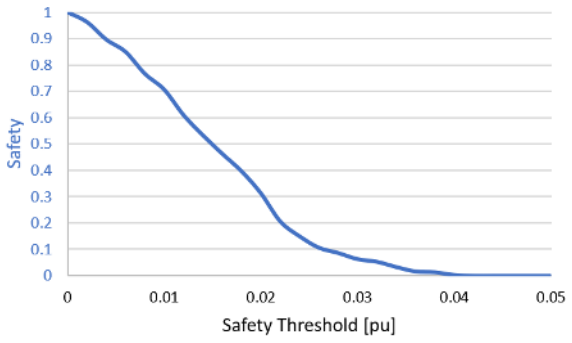

FIGURE 16. Safety $\bar{S}(x)$ on bus 33 for different threshold values.

It can be observed that some critical buses (for example, buses from 16 to 18, and from 31 to 33) are characterized by a high value of the safety metrics. Based on the presented definition of Safety (cfr. IV-A3), it means that these buses have a high probability of estimation error. The safety values are dependent both on the location of the measurement devices, and on the strict threshold adopted (0.02 *pu*). On Fig. 16 the

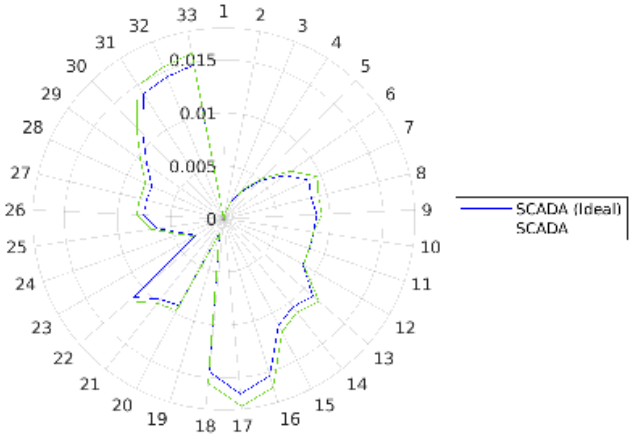

(a) Mean Estimation Error $\bar{E}(x)$

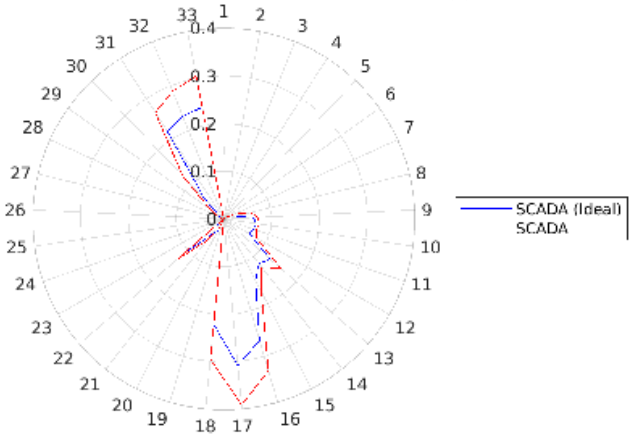

(b) Safety $\bar{S}(x)$

FIGURE 17. Comparison of SCADA-SE vs Ideal case.

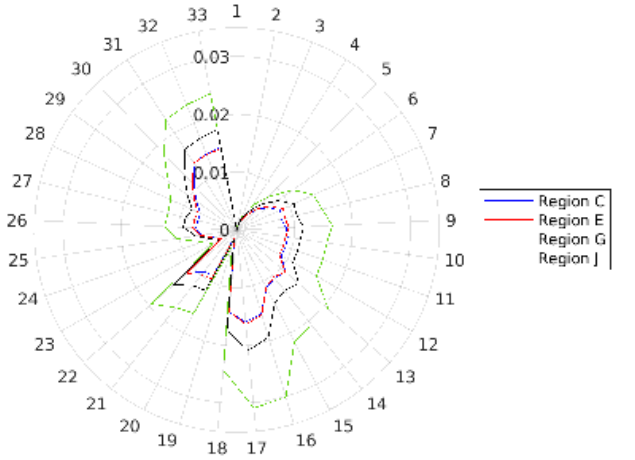

(a) Mean Estimation Error $\bar{E}(x)$

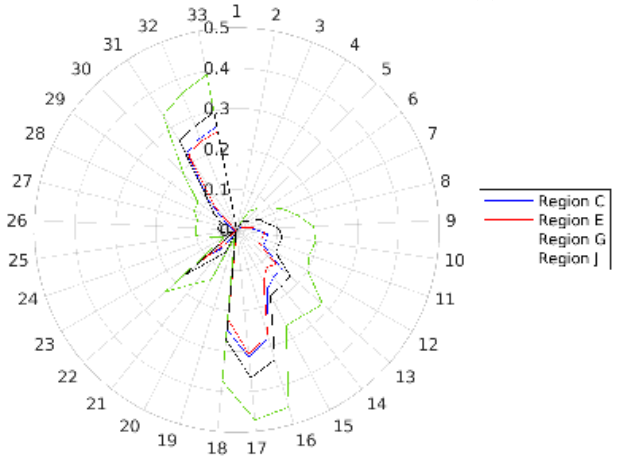

(b) Safety $\bar{S}(x)$

FIGURE 18. Comparison of the four rain regions of Norway.

safety metric is analyzed for different threshold values on bus 33. It can be observed that the safety decreases significantly for threshold values over 0.03 *pu*, becoming negligible for thresholds bigger than 0.04 *pu*.

Case B: This case focuses on analyzing the reliability of a 5G-based WAMS with traditional SCADA measurement installation. Figure 17a shows the comparison between the 5G-based WAMS with an ideal communication based (no failure) WAMS in terms of mean estimation error. It is observed that the mean estimation error, with the use of SCADA sensors, gives an error in the range of 0.5% to 1.5% in most of the buses. The results are close to the ideal case, where the errors are mainly due to uncertainty in the sensors data and the intrinsic accuracy of the estimator algorithm. Figure 17b shows the comparison among these two scenarios in terms of safety metrics. It can be observed that the probability of occurrence of critical state increases significantly in the 5G-based WAMS on buses 31 to 33, and 16 to 18, meanwhile on the other buses the safety metrics presents values similar to the ideal case.

Case B.1: The effect of rain on state estimation is studied for the four rain regions that intersect the Norway area (Table 2). On these cases, the state estimation calculation is based on a 5G-based SCADA system with traditional measurement devices. Figure 18a shows the mean estimation error metrics when there is rainfall. The simulation demonstrates the significance of rainfall rates on the accuracy of the state estimation. The rain region G has a significantly higher MER than other rain regions on all buses. The mean error ranges between 1.5% to 3% on a notable portion of the network (buses 31 to 33, 13 to 18) which might bring to major problems on power system operations. Even though, according to Table 2, region J presents a higher probability of rainfall, the mean estimation error for region J is lower than region G. This is due to the fact that region G has longer intense rainy periods, resulting in a significant attenuation. For most of the buses, the MER in region J ranges between 1% to 2%. For the other two areas which cover most of Norway, C and E, the introduced mean estimation error is relatively small, and the probability that rain introduces a significant attenuation is rare. The safety measures (Fig. 18b) show that all the regions considered have a significant probability of mean error greater than the threshold during rainy periods.

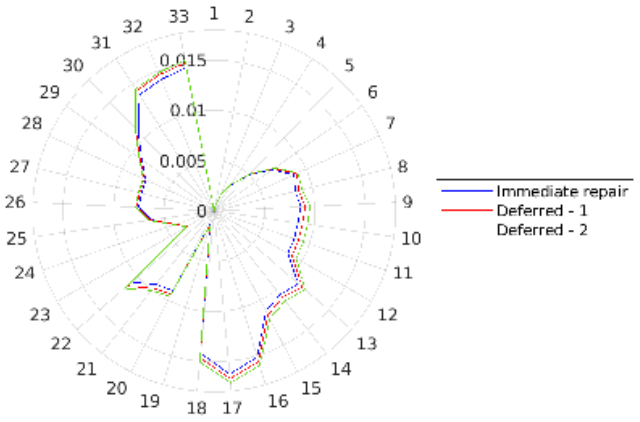

(a) Mean Estimation Error $\bar{E}(x)$

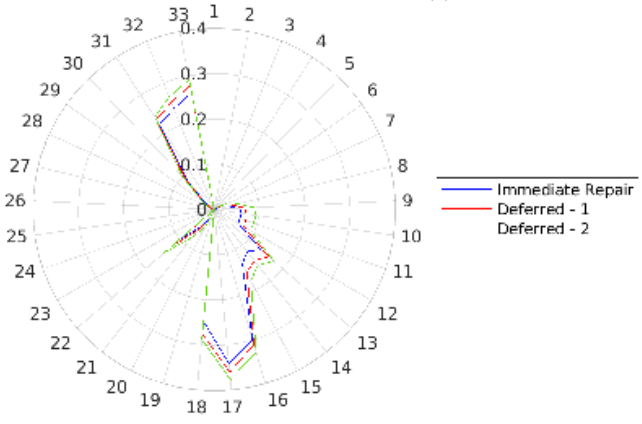

(b) Safety $\bar{S}(x)$

FIGURE 19. Comparison of repair strategies.

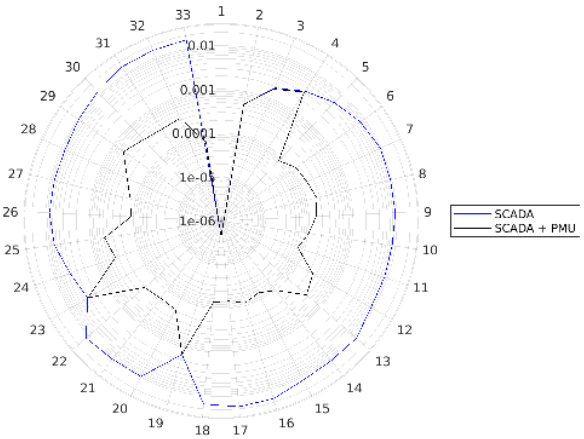

(a) Mean Estimation Error $\bar{E}(x)$

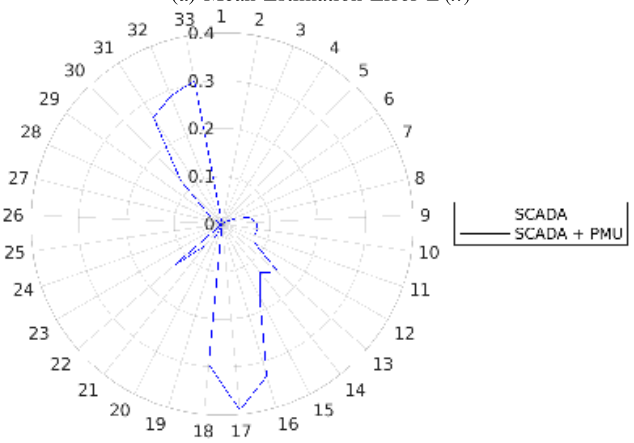

(b) Safety $\bar{S}(x)$

FIGURE 20. Comparison of SCADA-SE and (SCADA + PMU)-SE.

The region G appears to be the most critical in terms of probability of having a decisive action by the DMS due to the high mean estimation error.

Case B.2: A closer look at the impact of sensors failures with the use of different recovery strategies is shown in Fig. 19a and Fig. 19b. Figure 19a shows the polar plot of the mean estimation error for three scenarios: immediate repair; deferred repair until one other component fails; deferred repair until two other components fail. It can be seen that the effect of deferring the repair up to three components is small. This is mainly due to the use of pseudo measurements when measurement devices data are not received by the SCADA system: when the power load variations are relatively slow compared with the repair rates, the impact of sensors failures is in this context negligible.

Case C: The benefit in the adoption of a PMU-based state estimation is investigated in this case by comparing its performances with a traditional SCADA-based WLS state estimation. Figure 20a shows the mean estimation error comparison of the two 5G state estimation approaches: (SCADA + PMU)-SE and SCADA-SE. The results show a significant improvement in terms of MER with the PMU-based state estimation, compared with the traditional WLS state estimation. Note that in Fig. 20a the scale of magnitudes is logarithmic, hence the gain in MER reduction is more than two decades in a significant part of the network.

For some buses (such as bus 2-4, bus 19, bus 23), the two approaches give the same mean error, i.e. the use of μPMUs does not yield a significant improvement of the mean estimation error for these. This is mainly due to the placement of μPMUs on the topography considered.

The safety of the WAMS is also compared for the two state estimation approaches, and the results are shown in Fig. 20b. The estimations with μPMUs are seen as a dot in the origo. State estimation with standard measurement devices shows a significant probability that the MER can be higher than the 2 % threshold. Buses such as 16 to 18 and 31 to 33 have a relatively high probability of causing critical actions by the DMS (safety > 0.2), some buses such as 9 to 15 show safety metrics in the range of 0.1, and all the rest of the buses present an almost negligible probability. On the other hand, state estimation with μPMUs shows a very small probability that the error causes a wrong decision by the DMS. The (SCADA + PMU)-SE approach proves to be extremely accurate: the 10-year simulations reveal only one event where the mean estimation error exceeded the 2% threshold on one bus.

V. CONCLUSION

This paper has presented a novel methodological approach for analyzing the impact of 5G internal and external sources of interference to the ability of WAMS to provide measurement data to a Smart Grid state estimator. Different state estimator algorithms are compared, namely traditional WLS state estimator and PMU-based state estimator. The performance of these algorithms are compared in terms of Mean Estimation Error and Safety metrics.

The results obtained with the methodology proposed highlight the necessity of studying smart grids as cyber-physical systems to model and analyze the power system and the ICT system comprehensively. They also show how the failures in the ICT system may increase the intrinsic level of inaccuracy of measurement devices and state estimation algorithms.

The radio channel may be considerably affected by external factors such as fading and rain conditions. The outcome of the study indicates that this is the major cause of estimation error, affecting both state estimation MER and safety.

In the 5G-based WAMS scenario with traditional measurement devices, the mean estimation error along the grid buses is close to the ideal case, although there is a critical increase of probability that the estimation error may bring to wrong decisions by the DMS on some buses. The adoption of μPMUs measurement in the distribution network shows a significant improvement in the accuracy of the voltage estimation: the mean estimation error is reduced by more than two decades. The occurrence of wrong decisions by the DMS due to a high mean estimation error becomes negligible. The close-to-ideal behavior of 5G-URLLC observed in the dependability analysis enforces the prospect of a future adoption of 5G technologies for smart grid monitoring application, both for traditional SCADA- and PMU-based monitoring systems.

Tentative extension of this study as future work includes the analysis of the 5G technology as a service provider for power system monitoring and control. The study will focus on the effect of communication failures in the efficiency of a voltage regulation algorithm for distribution grids.

REFERENCES

[1] C. Legner, T. Eymann, T. Hess, C. Matt, T. Böhmann, P. Drews, A. Mädche, N. Urbach, and F. Ahlemann, "Digitalization: Opportunity and challenge for the business and information systems engineering community," *Bus. Inf. Syst. Eng.*, vol. 59, no. 4, pp. 301–308, 2017. [Online]. Available: http://link.springer.com/10.1007/s12599-017-0484-2

[2] C. Cecati, G. Mokryani, A. Piccolo, and P. Siano, "An overview on the smart grid concept," in *Proc. 36th Annu. Conf. IEEE Ind. Electron. Soc. (IECON)*, Nov. 2010, pp. 3322–3327.

[3] M. A. Rahman, E. Al-Shaer, and R. G. Kavasseri, "A formal model for verifying the impact of stealthy attacks on optimal power flow in power grids," in *Proc. ACM/IEEE Int. Conf. Cyber-Phys. Syst. (ICCPS)*, Apr. 2014, pp. 175–186.

[4] F. Aminifar, M. Fotuhi-Firuzabad, M. Shahidehpour, and A. Safdarian, "Impact of WAMS malfunction on power system reliability assessment," *IEEE Trans. Smart Grid*, vol. 3, no. 3, pp. 1302–1309, Sep. 2012.

[5] Y. Zhang, M. Larsson, B. Pal, and N. F. Thornhill, "Simulation approach to reliability analysis of WAMPAC system," in *Proc. IEEE Power Energy Soc. Innov. Smart Grid Technol. Conf. (ISGT)*, Feb. 2015, pp. 1–5.

[6] K. Zhu, M. Chenine, and L. Nordstrom, "ICT architecture impact on wide area monitoring and control Systems' reliability," *IEEE Trans. Power Del.*, vol. 26, no. 4, pp. 2801–2808, Oct. 2011.

[7] A. S. Rana, M. S. Thomas, and N. Senroy, "Reliability evaluation of WAMS using Markov-based graph theory approach," *IET Gener., Transmiss. Distrib.*, vol. 11, no. 11, pp. 2930–2937, Aug. 2017.

[8] Y. Liu, P. Ning, and M. K. Reiter, "False data injection attacks against state estimation in electric power grids," *ACM Trans. Inform. Syst. Secur.*, vol. 14, no. 1, p. 13, 2011. [Online]. Available: http://doi.acm.org/10.1145/1952982.1952995

[9] A. Ashok and M. Govindarasu, "Cyber attacks on power system state estimation through topology errors," in *Proc. IEEE Power Energy Soc. Gen. Meeting*, Jul. 2012, pp. 1–8.

[10] T. Cutsem, M. Ribbens-Pavella, and L. Mili, "Bad data identification methods in power system state Estimation–A comparative study," *IEEE Trans. Power App. Syst.*, vol. PAS-104, no. 11, pp. 3037–3049, Nov. 1985.

[11] G. Celli, P. A. Pegoraro, F. Pilo, G. Pisano, and S. Sulis, "DMS cyber-physical simulation for assessing the impact of state estimation and communication media in smart grid operation," *IEEE Trans. Power Syst.*, vol. 29, no. 5, pp. 2436–2446, Sep. 2014.

[12] A. Tsitsimelis, C. Kalalas, J. Alonso-Zarate, and C. Anton-Haro, "On the impact of LTE RACH reliability on state estimation in wide-area monitoring systems," in *Proc. IEEE Wireless Commun. Netw. Conf. (WCNC)*, Apr. 2018, pp. 1–6.

[13] M. Cosovic, A. Tsitsimelis, D. Vukobratovic, J. Matamoros, and C. Anton-Haro, "5G mobile cellular networks: Enabling distributed state estimation for smart grids," *IEEE Commun. Mag.*, vol. 55, no. 10, pp. 62–69, Oct. 2017.

[14] M. Cosovic, D. Vukobratovic, and V. Stankovic, "Linear state estimation via 5G C-RAN cellular networks using Gaussian belief propagation," in *Proc. IEEE Wireless Commun. Netw. Conf. (WCNC)*, Apr. 2018, pp. 1–6.

[15] D. Junce and C. Zexiang, "Mixed measurements state estimation based on wide-area measurement system and analysis," in *Proc. IEEE/PES Transmiss. Distrib. Conf. Expo., Asia Pacific*, Aug. 2005, pp. 1–5.

[16] M. Shahraeini and M. H. Javidi, "Wide area measurement systems," in *Advanced Topics in Measurements*. Rijeka, Croatia: IntecOpen, 2012, ch. 15. [Online]. Available: https://doi.org/10.5772/35466

[17] T. G. Dimon, *The Automation, Systems, and Instrumentation Dictionary*, 4th ed. Research Triangle Park, NC, USA: International Society of Automation, Oct. 2002.

[18] K. C. Budka, J. G. Deshpande, and M. Thottan, *Communication Networks for Smart Grids: Making Smart Grid Real*, 4th ed. London, U.K.: Springer, Feb. 2014.

[19] E. Kabalci and Y. Kabalci, *Smart Grids and Their Communication Systems*. Singapore: Springer, 2019.

[20] Y.-F. Huang, S. Werner, J. Huang, N. Kashyap, and V. Gupta, "State estimation in electric power grids: Meeting new challenges presented by the requirements of the future grid," *IEEE Signal Process. Mag.*, vol. 29, no. 5, pp. 33–43, Sep. 2012.

[21] A. Jain and S. Bhullar, "Micro-phasor measurement units (μ PMUs) and its applications in smart distribution systems," in *ISGW 2017: Compendium of Technical Papers* (Lecture Notes in Electrical Engineering). Singapore: Springer, 2018, pp. 81–92.

[22] A. von Meier, D. Culler, A. McEachern, and R. Arghandeh, "Micro-synchrophasors for distribution systems," in *Proc. ISGT*, Feb. 2014, pp. 1–5.

[23] M. Kuzlu, M. Pipattanasomporn, and S. Rahman, "Communication network requirements for major smart grid applications in HAN, NAN and WAN," *Comput. Netw.*, vol. 67, pp. 74–88, Jul. 2014. [Online]. Available: http://www.sciencedirect.com/science/article/pii/S1389128614001431

[24] J. Holmlund, "Working group on smart secondary substations technology development and distribution system benefits–CIRED's point of view–Final Report," in *Proc. CIRED Workshop*, 2017, pp. 1–58. [Online]. Available: http://rgdoi.net/10.13140/RG.2.2.23927.93605

[25] L. Hossenlopp, "Engineering perspectives on IEC 61850," *IEEE Power Energy Mag.*, vol. 5, no. 3, pp. 45–50, May 2007.

[26] T. Predojev, A. Al-Hezmi, J. Alonso-Zarate, and M. Dohler, "A real-time middleware platform for the smart grid," in *Proc. IEEE Online Conf. Green Commun. (OnlineGreenComm)*, Nov. 2014, pp. 1–6.

[27] J. Gao, J. Liu, B. Rajan, R. Nori, B. Fu, Y. Xiao, W. Liang, and C. L. P. Chen, "SCADA communication and security issues," *Secur. Commun. Netw.*, vol. 7, no. 1, pp. 175–194, Jan. 2014. [Online]. Available: https://onlinelibrary.wiley.com/doi/abs/10.1002/sec.698

[28] H. J. Zhou, C. X. Guo, and J. Qin, "Efficient application of GPRS and CDMA networks in SCADA system," in *Proc. IEEE PES Gen. Meeting*, Jul. 2010, pp. 1–6.

[29] D. A. Goel and R. S. Mishra, "Remote data acquisition using wireless-SCADA system," *Int. J. Eng.*, vol. 3, no. 1, pp. 58–65, 2009.
[30] S. Hopkins and E. Kalaimannan, "Towards establishing a security engineered SCADA framework," *J. Cyber Secur. Technol.*, vol. 3, no. 1, pp. 47–59, Mar. 2019, doi: 10.1080/23742917.2019.1590920.
[31] X. Foukas, G. Patounas, A. Elmokashfi, and M. K. Marina, "Network slicing in 5G: Survey and challenges," *IEEE Commun. Mag.*, vol. 55, no. 5, pp. 94–100, May 2017.
[32] F. Z. Yousaf, M. Bredel, S. Schaller, and F. Schneider, "NFV and SDN—Key technology enablers for 5G networks," *IEEE J. Sel. Areas Commun.*, vol. 35, no. 11, pp. 2468–2478, Nov. 2017. [Online]. Available: http://ieeexplore.ieee.org/document/8060513/
[33] B. Blanco, J. O. Fajardo, I. Giannoulakis, E. Kafetzakis, S. Peng, J. Pérez-Romero, I. Trajkovska, P. S. Khodashenas, L. Goratti, M. Paolino, E. Sfakianakis, F. Liberal, and G. Xilouris, "Technology pillars in the architecture of future 5G mobile networks: NFV, MEC and SDN," *Comput. Standards Interfaces*, vol. 54, pp. 216–228, Nov. 2017. [Online]. Available: http://www.sciencedirect.com/science/article/pii/S0920548916302446
[34] H. V. K. Mendis, P. E. Heegaard, and K. Kralevska, "5G network slicing for smart distribution grid operations," in *Proc. CIRED*, 2019, p. 5.
[35] *Elements for a Working Document Towards a Possible Preliminary Draft New Report on Utility Communication Systems*, ITU, document 5A/976-E, Annex 9, Geneva, Switzerland, Nov. 2018.
[36] F. Schweppe and J. Wildes, "Power system static-state estimation, part I: Exact model," *IEEE Trans. Power App. Syst.*, vol. PAS-89, no. 1, pp. 120–125, Jan. 1970.
[37] A. Abur and A. G. Expósito, *Power System State Estimation: Theory and Implementation*. Boca Raton, FL, USA: CRC Press, Mar. 2004.
[38] M. Zhou, V. A. Centeno, J. S. Thorp, and A. G. Phadke, "An alternative for including phasor measurements in state estimators," *IEEE Trans. Power Syst.*, vol. 21, no. 4, pp. 1930–1937, Nov. 2006.
[39] M. Simsek, A. Aijaz, M. Dohler, J. Sachs, and G. Fettweis, "5G-enabled tactile Internet," *IEEE J. Sel. Areas Commun.*, vol. 34, no. 3, pp. 460–473, Mar. 2016.
[40] W. H. Sanders and J. F. Meyer, "Stochastic activity networks: Formal definitions and concepts," in *Lectures on Formal Methods and PerformanceAnalysis* (Lecture Notes in Computer Science), vol. 2090. Berlin, Germany: Springer, 2001, pp. 315–343.
[41] S. Gaonkar, K. Keefe, R. Lamprecht, E. Rozier, P. Kemper, and W. H. Sanders, "Performance and dependability modeling with Möbius," *ACM SIGMETRICS Perform. Eval. Rev.*, vol. 36, no. 4, p. 16, 2009.
[42] T. Amare, M. Garau, and B. E. Helvik, "Dependability modeling and analysis of 5G based monitoring system in distribution grids," in *Proc. 12th EAI Int. Conf. Perform. Eval. Methodologies Tools (VALUETOOLS)*, 2019, pp. 163–166.
[43] D. Öhmann and G. P. Fettweis, "Minimum duration outage of wireless Rayleigh-fading links using selection combining," in *Proc. IEEE Wireless Commun. Netw. Conf. (WCNC)*, Mar. 2015, pp. 681–686.
[44] T. Hoesler, M. Simsek, and G. P. Fettweis, "Mission reliability for URLLC in wireless networks," *IEEE Commun. Lett.*, vol. 22, no. 11, pp. 2350–2353, Nov. 2018.
[45] *Characteristics of Precipitation for Propagation Modelling*, Recommendation document ITU-R 837-1, 1994.
[46] *Specific Attenuation Model for Rain for use in Prediction Methods*, Recommendation document ITU-R 838-3, 2005.
[47] M. E. Baran and F. F. Wu, "Network reconfiguration in distribution systems for loss reduction and load balancing," *IEEE Trans. Power Del.*, vol. 4, no. 2, pp. 1401–1407, Apr. 1989.
[48] J. Fan and S. Borlase, "The evolution of distribution," *IEEE Power Energy Mag.*, vol. 7, no. 2, pp. 63–68, Mar. 2009.
[49] R. T. Bhimarasetti and A. Kumar, "A new contribution to distribution load flow analysis for radial and mesh distribution systems," in *Proc. Int. Conf. Comput. Intell. Commun. Netw.*, Nov. 2014, pp. 1229–1236.
[50] T. Amare and B. E. Helvik, "Dependability analysis of smart distribution grid architectures considering various failure modes," in *Proc. IEEE PES Innov. Smart Grid Technol. Conf. Eur. (ISGT-Europe)*, Oct. 2018, pp. 1–6.
[51] T. Amare, C. M. Adrah, and B. E. Helvik, "A method for performability study on wide area communication architectures for smart grid," in *Proc. 7th Int. Conf. Smart Grid (icSmartGrid)*, Dec. 2019, pp. 64–73.
[52] D. S. Kim, J. B. Hong, T. A. Nguyen, F. Machida, J. S. Park, and K. S. Trivedi, "Availability modeling and analysis of a virtualized system using stochastic reward nets," in *Proc. IEEE Int. Conf. Comput. Inf. Technol. (CIT)*, Dec. 2016, pp. 210–218.
[53] D. S. Kim, F. Machida, and K. S. Trivedi, "Availability modeling and analysis of a virtualized system," in *Proc. 15th IEEE Pacific Rim Int. Symp. Dependable Comput.*, Nov. 2009, pp. 365–371.
[54] T. Amare, B. E. Helvik, and P. E. Heegaard, "A modeling approach for dependability analysis of smart distribution grids," in *Proc. 21st Conf. Innov. Clouds, Internet Netw. Workshops (ICIN)*, Feb. 2018.

TESFAYE AMARE ZERIHUN received the B.Sc. degree in electrical engineering from e Hawassa University, in 2011, and the M.Sc. degree in telematics from the Norwegian University of Science and Technology (NTNU), in 2015. He is currently pursuing the Ph.D. degree with the Department of Information Security and Communication Technology, NTNU. His main research interests include reliability and dependability analysis of future smart distribution grid as a system of systems, with main focus on the inter-dependency between the power systems and the ICT support systems.

MICHELE GARAU received the M.Sc. degree in energy engineering and the Ph.D. degree in industrial engineering from the University of Cagliari, in 2013 and 2018, respectively. He is currently a Postdoctoral Researcher with the Department of Information Security and Communication Technology, Norwegian University of Science and Technology (NTNU). His main research interests include dependability analysis of smart grids as cyber-physical systems, co-simulation of power and communication systems, and 5G communication for smart grid applications.

BJARNE E. HELVIK (Life Senior, IEEE) was born in 1952. He received the Siv.Ing. degree (M.Sc. in technology) and the Dr. Techn. degree from the Norwegian Institute of Technology (NTH), Trondheim, Norway, in 1975 and 1982, respectively. He has been a Professor with the Norwegian University of Science and Technology (NTNU), since 1997, and the Department of Telematics and Department of Information Security and Communication Technology. From 2009 to 2017, he was the Vice Dean with responsibility for research with the Faculty of Information Technology and Electrical Engineering, NTNU. He has previously held various positions at ELAB and SINTEF Telecom and Informatics. From 1988 to 1997, he was appointed as an Adjunct Professor with the Department of Computer Engineering and Telematics, NTH. His field of interests include QoS, dependability modeling, measurements, analysis and simulation, fault-tolerant computing systems and survivable networks, and related system architectural issues. His current research interests include ensuring dependability in services provided by multi-domain and virtualised ICT systems, with activities focusing on 5G and smartgrids.